

# Redshift evolution of clustering

Sabino Matarrese,<sup>1</sup> Peter Coles,<sup>2</sup> Francesco Lucchin<sup>3</sup> and Lauro Moscardini<sup>3</sup>

<sup>1</sup>*Dipartimento di Fisica G. Galilei, Università di Padova, via Marzolo 8, I-35131 Padova, Italy*

<sup>2</sup>*Astronomy Unit, School of Mathematical Sciences, Queen Mary & Westfield College, Mile End Road, London E1 4NS*

<sup>3</sup>*Dipartimento di Astronomia, Università di Padova, vicolo dell'Osservatorio 5, I-35122 Padova, Italy*

29 October 2021

## ABSTRACT

We discuss how the redshift dependence of the observed two–point correlation function of various classes of objects can be related to theoretical predictions. This relation involves first a calculation of the redshift evolution of the underlying matter correlations. The next step is to relate fluctuations in mass to those of any particular class of cosmic objects; in general terms, this means a model for the bias and how it evolves with cosmic epoch. Only after these two effects have been quantified can one perform an appropriate convolution of the non–linearly evolved two–point correlation function of the objects with their redshift distribution to obtain the ‘observed’ correlation function for a given sample. This convolution in itself tends to mask the effect of evolution by mixing amplitudes at different redshifts. We develop a formalism which incorporates these requirements and, in particular, a set of plausible models for the evolution of the bias factor. We apply this formalism to the spatial, angular and projected correlation functions from different samples of high–redshift objects, assuming a simple phenomenological model for the initial power–spectrum and an Einstein–de Sitter cosmological model. We find that our model is roughly consistent with data on the evolution of QSO and galaxy clustering, but only if the effective degree of biasing is small. We discuss the differences between our analysis and other theoretical studies of clustering evolution and argue that the dominant barrier to making definitive predictions is uncertainty about the appropriate form of the bias and its evolution with cosmic epoch.

**Key words:** cosmology: theory – cosmology: observations – large–scale structure of Universe – galaxies: formation – galaxies: evolution – galaxies: haloes

## 1 INTRODUCTION

The analysis of the clustering properties of various classes of objects at high redshift is rapidly becoming one of the key tests of models for the formation and present properties of the large–scale structure of the universe. The importance of such studies is that they offer the prospect of highlighting differences between viable theoretical models which, by construction, display clustering behaviour which is very similar at the present epoch (e.g. Coles 1996). Improvements in observational technology also offer the prospect of providing strong constraints on the nature of any bias that exists between the clustering of objects of a particular type and that of the underlying matter distribution. The possible existence of a significant bias in the galaxy distribution is a presently a significant obstacle, for example, to the determination of the cosmological density parameter  $\Omega_0$  from large–scale clustering data (e.g. Coles & Ellis 1996). This second point is particularly relevant because of the wide range of different objects which are now accessible to systematic redshift survey programmes - not only the ‘traditional’ bright, optically selected galaxies upon which surveys were based in the 1980s, but now also faint optical galaxies, galaxies selected in the infrared, QSOs, absorption–line systems, radio–galaxies and clusters of galaxies selected either optically or through their X–ray emission. Each of these classes of objects might be related to the matter distribution in a different way, a possibility

that, on the one hand, poses great difficulties of interpretation but, on the other, admits the possibility of realising many independent tests of theories for the formation of structure.

In spite of the many important recent observational developments, theoretical models used to interpret the data have so far generally been naive and poorly motivated in terms of galaxy formation scenarios. This theoretical inadequacy is clearly shown by the wide use, primarily in the literature relating to observational data, of the model

$$\xi(r, z) = \xi(r/(1+z), 0)(1+z)^{-(3+\epsilon)} \quad (1)$$

for the redshift evolution of the two-point correlation function  $\xi(r, z)$  at the comoving separation  $r$ , where  $\epsilon$  is an arbitrary fitting parameter. If the space dependence of the two-point function can be fitted by a power law, the above relation simplifies to

$$\xi(r, z) = (r/r_c)^{-\gamma}(1+z)^{-(3-\gamma+\epsilon)}, \quad (2)$$

where  $r_c$  is a constant measuring the unity crossing of  $\xi$  at  $z = 0$ .

Recent observational studies have served to highlight the importance of understanding the validity (or otherwise) of the simple models (1) & (2). For example, using equation (1) as a fitting formula for the two-point function of faint galaxies, various authors (e.g. Efstathiou et al. 1991; Neuschaefer, Windhorst & Dressler 1991; Couch, Jurcevic & Boyle 1993; Roche et al. 1993; Bernstein et al. 1994; Cole et al. 1994; Brainerd, Smail & Mould 1995; Le Fèvre et al. 1996; Roche et al. 1996; Shepherd et al. 1996) have found observational evidence for an excess evolution with respect to the stable clustering prediction ( $\epsilon = 0$ ), i.e. for positive values of  $\epsilon$  (the so-called *collapsing models*). In particular, Shepherd et al. (1996) and Le Fèvre et al. (1996), from the analysis of galaxy clustering at moderate redshifts, obtained  $\epsilon \sim 1 \pm 1$ . But is this a real (physical) discrepancy with realistic models, or would more sophisticated modelling of the evolution of  $\xi(r, z)$  yield a different interpretation? We incline to the second view, for reasons we explore below, and suggest that the quantity and quality of the high-redshift data now available requires a significant improvement in the mathematical models deployed for their interpretation.

In some ways this situation is reminiscent of the way some pre-COBE analyses of the CMB angular two-point function were carried out: in most experimental papers the data were fitted in terms of the so-called ‘Gaussian correlation function’, which had no justification in terms of theoretical models for the temperature anisotropy pattern. Likewise these simple power law models for the correlation function have relatively little theoretical motivation and a more realistic approach is consequently required.

Assuming that clustering grows by gravitational instability, the above formula is only justified in two cases: for  $\epsilon = 0$  it reproduces the prediction of the so-called *stable clustering* model, while, for  $\epsilon = n + 2 = \gamma - 1$ , it results from the application of linear theory in an Einstein–de Sitter universe to purely scale-free power-spectra,  $P_{\text{lin}}(k, 0) \propto k^n$ . The case where  $\epsilon = \gamma - 3$  corresponds to a clustering pattern that simply expands with the background cosmology as if the galaxies were just painted on a homogeneous background. Concerning the first case, one should remember that the idea underlying the stable clustering ansatz is that, on sufficiently small scales, gravity acts to stabilize the number of neighbours of an object in a proper volume, after this has turned around from the universal expansion. Although the physical grounds of this model appear to be reasonably sound (e.g. Jain & Bertschinger 1996 and references therein; see, however, Padmanabhan et al. 1996), numerical simulations indicate that this type of dynamics is only relevant on scales where the mass autocorrelation function is at least as large as  $\sim 100$  (e.g. Efstathiou et al. 1988), i.e. at most a small fraction of the typical scales probed by catalogues. The second model is also inadequate to treat the behaviour of correlation functions in any realistic galaxy formation scenario.

Melott (1992) has analysed the growth of clustering in numerical simulations for an ensemble of scale-free models. He finds that the lower is the value of the spectral index  $n$ , the larger is the value of the parameter  $\alpha \equiv 3 - \gamma + \epsilon$  and that positive values of  $\epsilon$  are easily allowed for in all models with  $n \leq 1$ . Melott’s explanation for such a fast clustering growth is as follows: stable clustering is not an upper limit to the growth of correlations; whenever the initial conditions contain non-vanishing large-scale power, merging makes new clusters form, their central density increases with time, which in turn enhances the growth of correlations. Using N-body simulations in the framework of the cold dark matter (CDM) model, Efstathiou (1995) has shown that faint blue galaxies can have lower correlation amplitude than normal luminous galaxies observed at the present day, as displayed by the observed value of  $\epsilon$ , provided that such faint galaxies are a transient population associated with dark matter haloes of low mass (less than  $\sim 10^{12} M_\odot$ ) and rotation speed. A numerical study of the evolution of the two-point function both for the matter and halo population has been recently carried out by Colín, Carlberg & Couchman (1996); they obtain a scale-dependent  $\epsilon$  parameter which is about 1 for mass particles in an Einstein–de Sitter universe, and lower for low-density models. A broad range of values (ranging from  $-0.2$  to  $1$  in the flat case and reaching lower values in the open case) is obtained for haloes, depending on their mean density (see also Brainerd & Villumsen 1994).

Recently, Jain (1996) has discussed the reliability of the general relation of equation (1) in the context of various models. His conclusions are that the above parameterization for the evolution of clustering is inaccurate in CDM-like

models, for two reasons. First, because the growth of  $\xi(r, z)$  with time on intermediate scales is much faster than the  $(1+z)^{-3}$  law prescribed by stable clustering at fixed proper separation (see also Peacock & Dodds 1996), second, because the boundary between the linear, mildly non-linear and stable clustering regimes, occurs at scales which rapidly change with time.

A major advance in this field was represented by the work of Hamilton et al. (1991), which first provided a sort of semi-analytic model (see also Nityananda & Padmanabhan 1994), able to interpolate between the very small-scale behaviour, accurately described by stable clustering, and the very large-scale (and/or early-time) one, which is expected to follow the simple prescriptions of linear perturbation theory. Of course, there also exist some more physically motivated models for non-linear gravitational clustering, such as the Zel'dovich approximation (Zel'dovich 1970) or alternative algorithms (e.g. Sahni & Coles 1995 for a recent review), like the adhesion (Gurbatov, Saichev & Shandarin 1989), frozen-flow (Matarrese et al. 1992) and frozen-potential (Brainerd, Scherrer & Villumsen 1993; Bagla & Padmanabhan 1994) approximations, which allow one to follow the time-evolution of the clustering of collisionless matter on a wide range of scales and epochs. However, in contrast to the Hamilton et al. (1991) ansatz and later modifications of it (Peacock & Dodds 1994; Jain, Mo & White 1995; Peacock & Dodds 1996), none of these alternative algorithms exactly reproduces the correct very small-scale (i.e. strongly non-linear) behaviour.

An approach similar to the one by Hamilton et al. (1991) has been applied by Peacock & Dodds (1994, 1996) in Fourier space to evolve the dimensionless power-spectrum (actually the contribution to the variance per unit  $\ln k$ ) into the non-linear regime. These types of approaches have been tested against numerical simulations in the linear and mildly non-linear regimes by Baugh & Gaztañaga (1996). Padmanabhan (1996), Bagla & Padmanabhan (1996), Padmanabhan et al. (1996) and Munshi & Padmanabhan (1996) have investigated the more strongly non-linear regime, the latter authors in particular questioning the applicability of the stable clustering limit. Sheth & Jain (1996) suggest that the limit of stable clustering on small scales is only expected to ensue on scales where the density contrast exceeds  $\sim 300 - 600$ . This issue remains controversial.

Besides the problems connected to the non-linear evolution of the clustering of the dark matter, one also has to face further non-trivial problems, such as the correct definition of the linear bias factor relating – in the simplest possible case – the object number-density fluctuations to the mass-density fluctuation field, and its redshift dependence. Although the idea that cosmic objects of different types might be biased is ubiquitous in modern cosmology, the models that have so far been constructed are relatively crude. This question is therefore one of the major stumbling blocks to further progress in the analysis of cosmological structure formation. The problem is particularly crucial here, for do we need to know not only the form of the bias at the present epoch but also its redshift-dependence.

One also has to take care to consider exactly how the ‘intrinsic’ redshift-dependent correlation function of any given class of objects is related to the ‘observed’ one, i.e. to the statistic one is actually able to extract from the data, which usually involves convolving with the redshift distribution of objects in the catalogue, accounting for the mask, correcting for redshift-space distortions and for the magnification bias induced by weak gravitational lensing, and finally adopting an appropriate choice for the redshift binning.

The main point we are making is that one needs to be very careful indeed about drawing conclusions on the behaviour of the intrinsic correlation function of the given objects and on the scenario of galaxy formation from the observed clustering of high-redshift objects, because of intervention of these difficulties. Constructing a theoretical framework for modelling these effects is the main task of this work. The plan of the paper is as follows. In Section 2 we define the ‘observed’ spatial, angular and projected two-point correlation function for high-redshift objects and discuss its connection with the underlying mass autocorrelation function. In Section 3 we present a theoretical model for the redshift evolution of the correlations of the underlying matter distribution. In Section 4 we introduce a generalized model for the bias of a class of objects and how the bias might evolve with epoch, discussing some special cases of this model in some detail. In Section 5 we apply our formalism to the clustering of QSOs and galaxies at high redshift. Conclusions are drawn in Section 6, where we also discuss the relationship of this work to alternative analyses of clustering evolution.

## 2 DESCRIPTION OF CLUSTERING

Let  $n_{\text{obs}}(x\hat{\gamma}; z, M)$  be the number-density of objects with redshift  $z$  that an observer placed in the origin measures in the angular direction specified by the unit vector  $\hat{\gamma}$ . Here  $x = x(z)$  is the comoving radial coordinate corresponding to the redshift  $z$ , which, in a matter dominated universe is given by Mattig’s formula (e.g. Peebles 1980)

$$x(z) = \frac{2c}{a_0 H_0} \frac{\Omega_0 z + (\Omega_0 - 2)[-1 + (\Omega_0 z + 1)^{1/2}]}{\Omega_0^2(1+z)} \equiv \frac{2cA(z)}{a_0 H_0 \Omega_0^2(1+z)}, \quad (3)$$

$\Omega_0$  being the density parameter and  $H_0$  the present value of Hubble’s constant. Note that, while in the Einstein-de Sitter case  $a_0$  is an arbitrary length-scale which can be set to unity, in the non-flat case it is given by

$$a_0 = \frac{c}{H_0} |1 - \Omega_0|^{-1/2}. \quad (4)$$

In order to convert dimensionless comoving coordinates to physical comoving ones, i.e. expressed in Mpc, one should always multiply by  $a_0$ ; so, for instance, the comoving radial distance of an object with radial coordinate  $x(z)$  is  $r(z) \equiv a_0 x(z)$ . The inverse relation of (3) is also useful:

$$1 + z(x) = 2 \frac{2y(1 - \Omega_0) + \Omega_0 + (2 - \Omega_0)[1 + y^2(1 - \Omega_0)]^{1/2}}{(2 - y\Omega_0)^2}, \quad y \equiv \frac{H_0 a_0 x}{c}. \quad (5)$$

In adopting the above relations we are implicitly assuming that redshift distortions are negligible, which is a good approximation in dealing with high redshift objects. The object number–density will generally also depend on other quantities such as mass, luminosity or absolute magnitude in a given wave–band, etc., which we generally indicated by the variable  $M$ ;  $n_{\text{obs}}(x\hat{\gamma}; z, M)$  will be taken to represent the observed number–density of objects per unit logarithmic interval of  $M$ . In the particular models discussed in Sec. 4, however, we shall make the assumption that relevant physical parameters of the object are tightly correlated with the halo mass and, in that context, we shall simply take  $M$  to mean the mass of the parent halo.

The probability per unit solid angle to observe an object of type  $M$  with redshift in the interval  $z, z + dz$  is

$$\int_{4\pi} \frac{d\Omega_\gamma}{4\pi} n_{\text{obs}}(x\hat{\gamma}; z, M) g(z) dz, \quad (6)$$

where

$$\begin{aligned} g(z) &\equiv a_0^3 (1+z)^{-3} \left[ 1 - \frac{(H_0 a_0 x)^2}{c^2} (\Omega_0 - 1) \right]^{-1/2} x^2 \frac{dx}{dz} \\ &= \frac{8c^3 A^2(z)}{H_0^3 \Omega_0^4 (1+z)^7} \left\{ 1 - \frac{4(\Omega_0 - 1)}{\Omega_0^2 (1+z)^2} A^2(z) \right\}^{-1/2} \left\{ \Omega_0 + (\Omega_0 - 2) \left[ 1 + \frac{\Omega_0(1+z)}{2(1+\Omega_0 z)^{1/2}} - (1+\Omega_0 z)^{1/2} \right] \right\}. \end{aligned} \quad (7)$$

The joint probability per squared unit solid angle to observe two objects of type  $M_1$  and  $M_2$  at redshifts  $z_1$  and  $z_2$  in directions separated by an angle  $\vartheta$  is

$$\int_{4\pi} \frac{d\Omega_{\gamma_1}}{4\pi} \frac{d\Omega_{\gamma_2}}{2\pi} \delta^D(\hat{\gamma}_1 \cdot \hat{\gamma}_2 - \cos \vartheta) n_{\text{obs}}(x_1 \hat{\gamma}_1; z_1, M_1) n_{\text{obs}}(x_2 \hat{\gamma}_2; z_2, M_2) g(z_1) g(z_2) dz_1 dz_2, \quad (8)$$

where  $\delta^D$  stands for the Dirac delta function.

In practice one calculates different quantities, namely the mean number of objects per unit solid angle with redshift in some range  $\mathcal{Z}$  and  $M$  in a certain domain  $\mathcal{M}$ ,

$$\bar{N}_\Omega = \int_{\mathcal{M}} d \ln M' \int_{\mathcal{Z}} dz' g(z') \int_{4\pi} \frac{d\Omega_\gamma}{4\pi} n_{\text{obs}}(x' \hat{\gamma}; z', M'), \quad (9)$$

and the mean number of pairs at fixed comoving separation  $r$  in the same redshift interval and  $M$  domain,

$$\bar{N}_{\text{pairs}}(r) \propto \int_{\mathcal{M}} d \ln M_1 d \ln M_2 \int_{\mathcal{Z}} dz_1 dz_2 g(z_1) g(z_2) \int_{4\pi} \frac{d\Omega_{\gamma_1}}{4\pi} \frac{d\Omega_{\gamma_2}}{2\pi} \delta^D(\hat{\gamma}_1 \cdot \hat{\gamma}_2 - \cos \vartheta(x_1, x_2, r)) n_{\text{obs}}(x_1 \hat{\gamma}_1; z_1, M_1) n_{\text{obs}}(x_2 \hat{\gamma}_2; z_2, M_2), \quad (10)$$

where  $\vartheta(x_1, x_2, r)$  is the angle between two sides of a triangle whose radial coordinates are  $x_1$  and  $x_2$ , given that the third side has size  $r \equiv a_0 x_{12}$ , as measured from the point with coordinate  $x_1$ . In a flat geometry,

$$\cos \vartheta(x_1, x_2, r) = \frac{x_1^2 + x_2^2 - x_{12}^2}{2x_1 x_2}, \quad (11)$$

while in the most general non–flat universe case the relation must be obtained by inverting the expressions reported below. The observed number of objects will generally differ from the real one by the catalogue selection function  $\phi(z, M)$ , which, for simplicity, we assume to be isotropic,  $n_{\text{obs}}(x\hat{\gamma}; z, M) = \phi(z, M) n(x\hat{\gamma}; z, M)$ , where  $n(x\hat{\gamma}; z, M)$  is the ‘real’ number density of objects. Once the selection function is known, the mean number of pairs in the sample can be compared with different realizations of a theoretical model, corresponding to different observers. In practice, however, it is easier to compare the observed number of pairs directly with the ensemble average of the same quantity in the theory. Angular brackets will denote ensemble averages (or averages over different spatial locations of the observer). The ensemble averaged mean number–density of objects of type  $M$  and redshift  $z$  will then be  $\bar{n}_{\text{obs}}(z, M) = \phi(z, M) \langle \bar{n}(z, M) \rangle$ . The two averages commute, but the ensemble averaged number–density is direction independent, so the further angular mean becomes unnecessary,  $\bar{n}_{\text{obs}}(z, M) = \phi(z, M) \langle n(\mathbf{x}; z, M) \rangle \equiv \phi(z, M) \bar{n}(z, M)$ . Similarly, the ensemble averaged mean number of pairs with comoving separation  $r$ ,  $\langle \bar{N}_{\text{pairs}}(r) \rangle$ , depends on the cross–correlation  $\phi(z_1, M_1) \phi(z_2, M_2) \langle n(x_1 \hat{\gamma}_1; z_1, M_1) n(x_2 \hat{\gamma}_2; z_2, M_2) \rangle$ : from the statistical homogeneity and isotropy of the

random field  $n(\mathbf{x}; z, M)$ , it follows that the quantity in angular brackets is unaffected by quasi-translations (e.g. Weinberg 1972, pg. 413) and rotations, so that its only spatial dependence can be on the separation  $R_{12}$  of the point  $(x_2, \hat{\gamma}_2)$  as measured from the point  $(x_1, \hat{\gamma}_1)$  (e.g. Osmer 1981; Shanks & Boyle 1994<sup>\*</sup>), namely

$$R_{12} = a_0 \left\{ D^2 x_1^2 + x_2^2 - 2Dx_1x_2\hat{\gamma}_1 \cdot \hat{\gamma}_2 \right\}^{1/2}, \quad (12)$$

where

$$D = \left[ 1 - y_1^2(\Omega_0 - 1) \right]^{1/2} + \frac{x_1}{x_2} \left[ 1 - (1 - y_2^2(\Omega_0 - 1))^{1/2} \right] \hat{\gamma}_1 \cdot \hat{\gamma}_2, \quad (13)$$

where  $y_i = H_0 a_0 x_i / c$ . Equation (12) reduces to the usual cosine rule,  $R_{12} = a_0 \sqrt{x_1^2 + x_2^2 - 2x_1x_2\hat{\gamma}_1 \cdot \hat{\gamma}_2}$  in the Einstein-de Sitter case. Notice that the formula (12) for  $R_{12}$  is not symmetric in  $x_1$  and  $x_2$ . This is, however, only important if  $D$  differs significantly from unity which effectively means that one is dealing with distances of order the curvature radius. Since in any case we expect correlations from objects at such large separations to be very weak (Stebbins & Caldwell 1995) it is possible to ignore this effect for reasonable cosmological models. One can then replace the above cross-correlation into the expression for  $\langle \bar{N}_{\text{pairs}}(r) \rangle$  and perform the angular integrations; the effect of the Dirac delta function will then be that of fixing  $R_{12} = r$ . By normalising to the expected number of Poisson pairs in the same sample, one obtains (an ensemble average estimate for) the correlation function actually measured in the sample, namely

$$\xi_{\text{obs}}(r) = N^{-2} \int_{\mathcal{Z}} dz_1 dz_2 \int_{\mathcal{M}} d \ln M_1 d \ln M_2 \mathcal{N}(z_1, M_1) \mathcal{N}(z_2, M_2) \langle \delta_n(\mathbf{x}_1; z_1, M_1) \delta_n(\mathbf{x}_2; z_2, M_2) \rangle, \quad (14)$$

where  $\delta_n(\mathbf{x}; z, M) \equiv [n(\mathbf{x}; z, M) - \bar{n}(z, M)]/\bar{n}(z, M)$ , while  $\mathbf{x}_2$  is any point whose separation from  $\mathbf{x}_1$  is  $r$ . We also introduced the quantity  $\mathcal{N}(z, M) \equiv 4\pi g(z)\phi(z, M)\bar{n}(z, M)$ , representing the number of objects in the sample with intrinsic property  $M$  in the range  $(\ln M, \ln M + d \ln M)$  and redshift in the range  $(z, z + dz)$ , and its integrals  $\mathcal{N}(z) \equiv \int_{\mathcal{M}} d \ln M' \mathcal{N}(z, M')$  and  $N \equiv \int_{\mathcal{Z}} dz' \mathcal{N}(z')$ , with obvious physical interpretation. Given our assumptions, negligible redshift distortions and an isotropic selection function, the latter formula is exact and general. It shows that, in principle, one should know the cross-correlation of the random field  $n(\mathbf{x}; z, M)$  at two different  $z$  and  $M$ . In order to proceed, however, we need to make some approximations. First of all we will assume separation of property  $M$  and position in the form of a linear biasing factor relating the object number-density fluctuation  $\delta_n$  to the mass-density fluctuation  $\delta_m$ , namely  $\delta_n(\mathbf{x}; z, M) \approx b(M, z)\delta_m(\mathbf{x}; z)$ , which is a reasonable approximation as long as a calculation of the two-point function is concerned. In such a case we find

$$\xi_{\text{obs}}(r) = N^{-2} \int_{\mathcal{Z}} dz_1 dz_2 \mathcal{N}(z_1) \mathcal{N}(z_2) b_{\text{eff}}(z_1) b_{\text{eff}}(z_2) \langle \delta_m(\mathbf{x}_1; z_1) \delta_m(\mathbf{x}_2; z_2) \rangle, \quad (15)$$

where, again,  $\mathbf{x}_2$  is any point whose distance from  $\mathbf{x}_1$  is  $r$ , and we introduced the *effective* bias factor

$$b_{\text{eff}}(z) \equiv \mathcal{N}(z)^{-1} \int_{\mathcal{M}} d \ln M' b(M, z) \mathcal{N}(z, M') = \frac{\int_{\mathcal{M}} d \ln M' b(M, z) \phi(z, M') \bar{n}(z, M')}{\int_{\mathcal{M}} d \ln M' \phi(z, M') \bar{n}(z, M')}. \quad (16)$$

In fact, in a wide class of biasing scenarios one expects the bias parameter to be a monotonically decreasing function of scale (Coles 1993), so that the shape of the correlation function of objects at small scales is expected to be steeper than that of the mass. However, for simplicity we shall neglect this point in the subsequent analysis and assume that the bias can be described by a constant multiplier of the matter correlation function. We discuss the importance of bias in the study of clustering evolution at length in Section 4.

Next, we make the approximation that the dominant contribution to the integral in equation (15) comes from points whose redshifts are nearly the same. As far as the integral is concerned, we can then make the replacement  $\langle \delta_m(\mathbf{x}_1; z_1) \delta_m(\mathbf{x}_2; z_2) \rangle \rightarrow \xi(r, z_{\text{ave}})$ , where  $\xi(r, z_{\text{ave}})$  is the mass autocorrelation function at some intermediate redshift  $z_{\text{ave}}$  which we can take as  $z_{\text{ave}} = \bar{z} \equiv (z_1 + z_2)/2$ .<sup>†</sup> A rough criterion for the validity of this approximation is  $|\xi''(r, z)/\xi(r, z)|\Delta z^2 \ll 1$ , having indicated by a prime the differentiation with respect to  $z$ , where  $\Delta z$  is the width of the given redshift range; this point is discussed in more detail by Porciani (1996, in preparation). At this level the possible spatial curvature of the universe can be assumed to affect  $\xi(r, z)$  only through its time-evolution, since the comoving separation of any correlated pairs at the same redshift is certainly much smaller than the curvature length. We can then write

\* The formulae given by Shanks & Boyle (1994) contain two errors: first, their comoving radial coordinates are incorrectly normalised, which leads to wrong determinations of the object separations for any  $\Omega_0 \neq 0, 1$ ; second,  $D$  is incorrectly defined as the square root of the true one.

† Estimating  $z_{\text{ave}}$  through  $z(\bar{x})$  instead of  $\bar{z}$  would imply a negligible correction in the final integral (actually less than a few percent for separations larger than one Mpc, in the model considered below).

$$\xi(r, z) = \frac{1}{2\pi^2} \int_0^\infty dk k^2 P(k, z) j_0(kr), \quad (17)$$

with  $P(k, z)$  the mass fluctuation power-spectrum at  $z$ . The symbol  $j_\ell$  will be generally used to denote the spherical Bessel functions of order  $\ell$ . We then arrive to the simple expression

$$\xi_{\text{obs}}(r) = N^{-2} \int_{\mathcal{Z}} dz_1 dz_2 \mathcal{N}(z_1) \mathcal{N}(z_2) b_{\text{eff}}(z_1) b_{\text{eff}}(z_2) \xi(r, \bar{z}). \quad (18)$$

The observed correlation function in a given redshift interval is a suitable weighting of the mass autocorrelation function with the mean number of objects and effective bias factor in that range. Only in the limiting case where the objects belong to a narrow redshift interval one is allowed to approximate  $\xi_{\text{obs}}$  by the linear relation  $\xi_{\text{obs}}(r, z) \approx b_{\text{eff}}^2(z) \xi(r, z)$ , where  $z$  is the median redshift of the sample.

Using similar reasoning we can write a simple expression for the observed angular correlation function in a certain redshift interval and  $M$  domain, in terms of the mass autocorrelation function. The result is an extension of the relativistic Limber's formula (e.g. Peebles 1980, Sect. 56), accounting for a linear bias factor in the relation between  $\delta_n$  and  $\delta_m$ . One gets

$$\omega_{\text{obs}}(\vartheta) = N^{-2} \int_{\mathcal{Z}} dz_1 dz_2 \mathcal{N}(z_1) \mathcal{N}(z_2) b_{\text{eff}}(z_1) b_{\text{eff}}(z_2) \xi(r_{12}, z_{\text{ave}}), \quad (19)$$

where, neglecting the curvature corrections,  $r_{12} = a_0 \sqrt{x^2(z_1) + x^2(z_2) - 2x(z_1)x(z_2) \cos \vartheta}$ , with  $x(z)$  given by Matig's formula, equation (3). Adopting as usual the *small-angle* approximation, one can easily obtain the handier form

$$\omega_{\text{obs}}(\vartheta) = N^{-2} \int_{\mathcal{Z}} dz G(z) \mathcal{N}^2(z) b_{\text{eff}}^2(z) \int_{-\infty}^{\infty} du \xi(r(u, \vartheta, z), z), \quad (20)$$

where  $r(u, \vartheta, z) \equiv a_0 \sqrt{u^2 + x^2(z) \vartheta^2}$ , with  $x(z)$  given once again by equation (3), and

$$G(z) \equiv \left( \frac{dx}{dz} \right)^{-1} = \frac{a_0 H_0 \Omega_0^2 (1+z)^2}{2c} \left\{ \Omega_0 + (\Omega_0 - 2) \left[ 1 + \frac{\Omega_0(1+z)}{2(\Omega_0 z + 1)^{1/2}} - (\Omega_0 z + 1)^{1/2} \right] \right\}^{-1}. \quad (21)$$

Here the approximation of replacing the two redshift dependence of the mass autocorrelation function by a single intermediate redshift  $z_{\text{ave}}$  corresponds to the standard procedure (e.g. Peebles 1980, p. 215).

Another useful quantity to consider is the *projected* real-space correlation function for objects in the redshift band  $\mathcal{Z}$ . This statistic can be easily obtained by applying directly the Davis & Peebles (1983) technique to our  $\xi_{\text{obs}}(r)$  above. Defining  $r_p$  as the separation of a pair perpendicular to the line of sight,  $r_p = (r_1 + r_2) \tan(\vartheta_{12}/2)$ , with  $r_1$  and  $r_2$  the comoving radial coordinates of the members and  $\vartheta_{12}$  their angular separation, one simply has

$$w_{\text{obs}}(r_p) = 2 \int_0^\infty dy \xi_{\text{obs}}(\sqrt{r_p^2 + y^2}) = 2 \int_{r_p}^\infty dr r (r^2 - r_p^2)^{-1/2} \xi_{\text{obs}}(r). \quad (22)$$

In deriving this formula we have neglected peculiar motions, which, however, mostly affect separations along the line of sight, and assumed Euclidean geometry, which is a reasonable approximation as long as the underlying cross-correlation function is evaluated at a common mean redshift, as in equation (18).

As recently pointed out by Villumsen (1995), if the redshift distribution of faint galaxies is estimated by applying an apparent magnitude selection criterion, then there is a possibility that a magnification bias due to weak gravitational lensing (Turner 1980) would intervene in the relation between the intrinsic spatial correlation function and the observed angular one. A similar problem could also affect the observed spatial correlation function of high redshift objects. This effect has not been taken into account in this work but we note that it would tend to increase the observed correlation function of high-redshift objects by adding a source of extra apparent correlations over and above that produced by intrinsic spatial correlations of the objects themselves.

### 3 MODELLING THE EVOLUTION OF MATTER CORRELATIONS

In the light of the preceding discussion it is clear that a theory capable of predicting the observed correlation function of some class of objects must first incorporate a model for the initial linear autocorrelation function of the primordial density fluctuations and also a model describing how these correlations evolve with time. Only after this has been constructed does it make sense to worry about how a given class of objects relates to the mass distribution. We defer discussion of this second task to section 4; in this section we concentrate exclusively on the evolution of matter correlations.

As an illustrative example to which we shall apply our method, we assume the phenomenological linear power-spectrum obtained by Peacock & Dodds (1996) by fitting correlation results coming from different samples of galaxies and clusters. In their analysis they consider a linear power-spectrum of the form

$$P_{\text{lin}}(k, 0) = P_0 k^n T^2(k) , \quad (23)$$

with the CDM transfer function, as given by Bardeen et al. (1986),

$$T(k) = \frac{\ln(1 + 2.34q)}{2.34q} [1 + 3.89q + (16.1q)^2 + (5.46q)^3 + (6.71q)^4]^{-1/4} , \quad (24)$$

and  $q \equiv (k/h\text{Mpc}^{-1})/\Gamma_{\text{eff}}$ , where  $h$ , as usual, is the Hubble constant in units of  $100 \text{ km s}^{-1} \text{ Mpc}^{-1}$ . Peacock & Dodds (1996) find the following good fit for the effective shape parameter  $\Gamma_{\text{eff}} = 0.255 \pm 0.017 + 0.32(1/n - 1)$  originally introduced by Efstathiou, Bond & White (1992). In CDM models  $\Gamma_{\text{eff}}$  is related to the density parameter  $\Omega_0$  and to the baryonic fraction  $\Omega_b$  by the relation (Sugiyama 1995)  $\Gamma_{\text{eff}} = \Omega_0 h \exp[-\Omega_b(1 + 1/\Omega_0)]$ . White et al. (1996) have recently discussed critical-density CDM models with high baryon content, as suggested by recent observations, which would help to reduce  $\Gamma_{\text{eff}}$  below the ‘standard’ value of 0.5. In the following analysis, however, we take  $\Gamma_{\text{eff}} = 0.25$  as an empirical parameter, without any relation to a true CDM model, assuming  $\Omega_0 = 1$ .

The normalisation is then fixed consistently with the 4-year COBE data which give  $Q_{\text{rmsPS}} = 18 \pm 1.6 \mu\text{K}$  (Bennett et al. 1996; Górski et al. 1996), for  $n = 1$ , which we assume here, and  $T_0 = 2.728 \pm 0.004 \text{ K}$  (Fixsen et al. 1996). This leads to  $P_0 \approx 6.74 \times 10^5 (h^{-1} \text{ Mpc})^4$  and  $\sigma_8 \equiv \sigma_{\text{lin}}(8 h^{-1} \text{ Mpc}) = 0.65$ , in reasonably good agreement with the Peacock & Dodds (1994) amplitude. A more recent analysis of the COBE 4-year data by Bunn & White (1996), who used a Karhunen-Loève expansion to produce an unbiased estimate of the normalisation, implies an increase in the amplitude of the power-spectrum of order 16 per cent for a standard CDM model; but changing the normalisation of our phenomenological model in this way will not alter the conclusions of this paper.

The question of how the matter correlations evolve into the non-linear regime has been the subject of considerable recent research activity. A large fraction of the literature on the clustering of high-redshift objects uses either the self-similarity relation for stable clustering or *ad hoc* generalizations of it, as in equations (1) and (2), which also assume separation of the spatial (in proper coordinates) and redshift dependence (e.g. Peebles 1980). The self-similarity relation, obtained from equation (2) with  $\epsilon = 0$  (e.g. Peebles 1980), is expected to be the asymptotic state resulting from the evolution of scale-free initial conditions,  $P_{\text{lin}}(k, 0) \propto k^n$  ( $-3 < n < 4$ ), in an Einstein-de Sitter universe, and leading to  $\gamma = 3(3 + n)/(5 + n)$ . For more general initial power-spectra, the first relation, with  $\epsilon = 0$ , should still be valid in the stable clustering regime. However, it is well known that stable clustering describes the evolution of the mass autocorrelation function only in the strongly non-linear limit,  $\xi \gtrsim 100$  (e.g. Efstathiou et al. 1988), under the hypothesis that the peculiar relative velocity of the pair exactly balances the Hubble flow to form a bound configuration. This model only applies on very small scales (e.g. Efstathiou et al. 1988). On the other extreme, one has the linear theory prediction

$$\xi_{\text{lin}}(r, z) = D_+^2(z) \xi(r, 0) , \quad (25)$$

where  $D_+(z)$  is the growing mode of linear perturbations [ $D_+(z) = (1 + z)^{-1}$  in an Einstein-de Sitter model], which only applies to large scales and/or at early times, i.e. when  $\xi \ll 1$ . Scale-free initial conditions linearly evolved in an Einstein-de Sitter universe lead to the form of equation (2), with  $\epsilon = n + 2$  and  $\gamma = n + 3$ .

What one really needs is a model able to smoothly interpolate among the two above regimes, so that it can be safely applied in the mildly non-linear regime, i.e. that relevant for most objects at the relevant separations. Following Hamilton et al. (1991), various authors have recently obtained fits of the N-body results of the type

$$\bar{\xi}(r, z) = B(n_{\text{eff}}) F[\bar{\xi}_{\text{lin}}(r_0, z)/B(n_{\text{eff}})] , \quad r_0 = [1 + \bar{\xi}(r, z)]^{1/3} r , \quad (26)$$

where

$$\bar{\xi}(r, z) \equiv \frac{3}{r^3} \int_0^r y^2 \xi(y, z) dy = \frac{3}{2\pi^2 r} \int_0^\infty dk k P(k, z) j_1(kr) , \quad (27)$$

and similarly for  $\bar{\xi}_{\text{lin}}$  in terms of the linear power-spectrum,  $P_{\text{lin}}(k, z) = D_+^2(z) P_{\text{lin}}(k, 0)$ . In Hamilton et al. (1991) the  $B(n_{\text{eff}})$  factor was set to unity. For the Einstein-de Sitter case, Jain et al. (1995, hereafter JMW) gave theoretical arguments for  $B(n_{\text{eff}}) \approx (1 + n_{\text{eff}}/3)^{0.8}$ , with  $n_{\text{eff}}$  the effective spectral index, which for a general, i.e. non-scale-free, initial power-spectrum is defined as

$$n_{\text{eff}}(z) = \left. \frac{d \ln P_{\text{lin}}(k, z)}{d \ln k} \right|_{k=k_{nl}(z)} , \quad (28)$$

where  $k_{nl}^{-1}$  is the radius of a top-hat window function at which the *rms* linear mass fluctuation is unity. The JMW formula, which reads

$$F(X) = \frac{X + 0.45X^2 - 0.02X^5 + 0.05X^6}{1 + 0.02X^3 + 0.003X^{9/2}}, \quad X = \bar{\xi}_{\text{lin}}(r_0, z)/B(n_{\text{eff}}), \quad (29)$$

fits the N-body results, in the range of scales and redshifts where it is testable, with an accuracy better than twenty per cent. The JMW fit seems to perform better than the others (Hamilton et al. 1991; Peacock & Dodds 1994, 1996) in the highly non-linear regime, which is relevant if one needs to predict the amount of clustering at early epochs (e.g. Baugh & Gaztañaga 1996). The formula (29) differs from that used by Peacock & Dodds (1996) slightly in the asymptotic behaviour for small separations.

Here the linear prediction is obtained for  $X \rightarrow 0$ , while the stable clustering behaviour is asymptotically recovered for  $X \rightarrow \infty$ . To obtain the differential correlation function,  $\xi(r, z)$ , we need to differentiate the above relation with respect to  $r$ . We obtain

$$\xi(r, z) = \frac{[1 + B(n_{\text{eff}})F(X)]F'(X)\Delta\xi_{\text{lin}}(r_0, z)}{1 + B(n_{\text{eff}})F(X) - F'(X)\Delta\xi_{\text{lin}}(r_0, z)} + B(n_{\text{eff}})F(X), \quad (30)$$

with  $F' \equiv dF/dX$  and

$$\Delta\xi_{\text{lin}}(r_0, z) \equiv \xi_{\text{lin}}(r_0, z) - \bar{\xi}_{\text{lin}}(r_0, z) = \frac{1}{2\pi^2} \int_0^\infty dk k^2 P_{\text{lin}}(k, z) [j_0(kr_0) - (3/kr_0)j_1(kr_0)]. \quad (31)$$

In Fig. 1 we show the mass autocorrelation function  $\xi(r, z)$  obtained from the model above and compare it with the linear theory and stable clustering predictions for the same linear power-spectrum. Note that the stable clustering model always tends to largely overestimate the amplitude of the correlation function on quasi-linear scales.

The qualitative effect of convolving the intrinsic object correlation function  $b_{\text{eff}}^2(z)\xi(r, z)$  with the redshift distribution  $\mathcal{N}(z)$ , as prescribed by equation (18), can be that of partially diluting the signal. Quantitatively the effect can be estimated by using a very simple model: we assume no bias,  $b = 1$ , uniform selection function,  $\phi(z, M) = \text{constant}$ , and constant comoving object number-density,  $\mathcal{N}(z) \propto (1+z)^3 g(z)$ . Integration over a typical redshift range  $\Delta z = 2$ , centered on a median redshift of 1, shows that the observed correlation function systematically underestimates the intrinsic one by about ten per cent. The effect can be higher in case the redshift-dependence of either the catalogue selection function, or of the intrinsic object number-density, preferentially selects lower redshift objects, which are generally less biased.

An extension of this formalism to the open universe case has been obtained for the evolved power-spectrum in terms of the linear one by Peacock & Dodds (1996). The simple idea behind their extension is that if collapse occurs at high redshift, when  $\Omega$  was very close to unity, then non-linear correlations at fixed proper separation still evolve as  $(1+z)^{-3}$  at low redshift, what changes instead is the linear growth factor which is suppressed by a known  $\Omega$ -dependent factor. We shall defer discussion of clustering in open universe models to a later paper.

#### 4 EVOLUTION OF BIAS

We now turn to the issue of how objects trace the mass distribution, i.e. to the question of the bias and how it might evolve with epoch. In the framework we are considering here this basically boils down to the behaviour of the linear bias parameter  $b$ , where  $b^2$  is the factor by which the two-point correlation function of a given class of objects exceeds the autocorrelation function of the mass fluctuations. The clustering of observable objects is more difficult to model satisfactorily than that of their parent haloes, being sensitive to various cosmological and astrophysical effects as well as to the mass – or any other intrinsic property – dependence of the selection function. There are various possibilities as to how such a bias might originate, and different biasing schemes are expected to introduce a bias that depends on redshift in different ways. In this paper we shall discuss *four* simple models which incorporate evolutionary effects in a relatively straightforward way.

The first model we consider is the trivial one in which objects trace the mass at all epochs or, in terms of the bias parameter, that  $b = 1$  for all values of  $z$ . We shall use this model as a kind of reference standard against which to compare the behaviour of other, more complicated biasing scenarios. For short, we shall call this the *unbiased model*.

The next two models we consider are motivated by a recent discussion by Mo & White (1995) who, working within the Press-Schechter (1974) formalism, obtained an approximate formula (expected to be valid at large separations) for the linear bias relating the correlation function of dark matter haloes of mass  $M$  to that of mass-density fluctuations. As we mentioned in Sec. 2, we now assume that physical parameters of the objects forming in haloes of mass  $M$  are tightly correlated with  $M$ , so that the general ‘type’ parameter we used there ( $M$ ) is now taken to mean the mass of the parent halo. The assumption that the mass of the host halo determines the parameters of the object it contains may not be correct in detail, but it does allow the construction of relatively simple models that illustrate the way our formalism works. What emerges from these arguments is an expression for the bias parameter of dark matter haloes of mass  $M$  at redshift  $z$ , which formed at redshift  $z_f$ . The Mo & White (1985) formula reads

$$\xi_{\text{halo}}(r, z, M) = b^2(M, z|z_f)\xi(r, z), \quad (32)$$

with

$$b(M, z|z_f) = 1 + \frac{1}{\delta_f}(\nu_f^2 - 1) \quad (33)$$

in which  $\nu_f = \delta_f/\sigma_{\text{lin}}(z, M)$  and  $\delta_f = \delta_c D_+(z)/D_+(z_f)$ . Here  $\delta_c$  is the critical linear overdensity for spherical collapse ( $\delta_c = 1.69$  in the Einstein–de Sitter case), and  $\sigma_{\text{lin}}^2$  is the linear mass–variance at redshift  $z$  filtered in a sharp–edged sphere containing the mean mass  $M$ . The expression (33) implies a minimum value for the bias factor  $b(M, z|z_f) \geq 1 - 1/\delta_c$  (0.41 for  $\Omega_0 = 1$ ). The most relevant feature of this formula in this context is that it predicts  $b \approx 1$  at  $\nu_f = 1$ , which for  $\bar{n}(z, M)$  represented by the Press–Schechter mass–function,

$$\bar{n}(z, M) d \ln M = \sqrt{\frac{2}{\pi}} \frac{\bar{\rho}_0(1+z)^3}{M D_+(z) \sigma_{\text{lin}}(0, M)} \left| \frac{d \ln \sigma_{\text{lin}}(0, M)}{d \ln M} \right| \exp \left[ -\frac{\delta_c^2}{2 D_+^2(z) \sigma_{\text{lin}}^2(0, M)} \right] d \ln M, \quad (34)$$

(with  $\bar{\rho}_0$  the mean mass density at  $z = 0$ ), roughly corresponds to the peak mass  $M_*(z_f)$ , implicitly defined by  $\sigma_{\text{lin}}(z_f, M_*) = \delta_c/\sqrt{2}$ . We are interested not in  $b(M, z|z_f)$  but the bias of all haloes of mass  $M$  that exist at an epoch  $z$ , which we call  $b(M, z)$ . This latter quantity is, in principle, obtained by integrating equation (33) over all  $z_f \geq z$  taking into account the relevant *survival probability* of a halo of mass  $M$  formed at  $z_f$  not being destroyed by merging by the epoch  $z$ . It is, however, implicit in the Press–Schechter approach that the only objects that exist at any epoch  $z$  are those which have just formed by the merging of smaller mass units (Sahni & Coles 1995, Sec. 3.4). This assumption may be questionable, but it is nevertheless consistent, within the Press–Schechter formalism, to argue that  $b(M, z) = b(M, z|z_f = z)$ . Looked at in this way, the formula (33) leads to the result one would expect from the so–called peak–background split (Efstathiou et al. 1988; Cole & Kaiser 1989), and reduces to the standard form  $b \approx \delta_c/\sigma^2$  in the limit of high peaks (Kaiser 1984), implying a  $D_+^{-2}(z)$  (i.e.  $(1+z)^2$  if  $\Omega_0 = 1$ ) redshift dependence in such a limit.

The task of obtaining the form of  $b(M, z)$  for objects undergoing dissipative collapse, such as galaxies, is rather more involved than just finding this function for their haloes. While haloes may merge rapidly and lose their identity, the same is not necessarily true for the galaxies they contain. For this reason, Mo, Jing & White (1996) prefer to use the formula (33) for pairs of galaxy clusters with separations  $r \geq 10 h^{-1}$  Mpc, assuming that a cluster can indeed be thought of as a single large halo, despite the fact that it contains many separate galaxies. There is therefore some ambiguity in how to translate the formula (33) to a specific situation of a particular class of objects.

One way to incorporate the above formulae into a model for the observed clustering of objects is to assume that one can observe all haloes exceeding a certain cutoff mass  $M_{\text{min}}$  at any particular redshift, i.e.  $\phi(z, M) = \Theta(M - M_{\text{min}})$  at any  $z$ , where  $\Theta(\cdot)$  is the Heaviside step function. One then has to weight the correlation function of haloes of mass  $M$  by the appropriate number density. We can thus model the linear bias at redshift  $z$  for haloes of mass  $M$  as in equation (33) and get the redshift evolution of the effective bias factor  $b_{\text{eff}}(z)$  through equation (16), by weighting it consistently with the Press–Schechter mass–function  $\bar{n}(z, M)$ . A plot of  $b_{\text{eff}}(z)$  for different choices of the minimum cutoff mass in  $\bar{n}(z, M)$  is shown in Fig. 2. The  $z$ –dependence of  $b_{\text{eff}}$  changes with  $M_{\text{min}}$ , which also determines its present value, with the constant value 0.41, obtained for  $M_{\text{min}} \rightarrow 0$ . (Note that, in principle,  $M_{\text{min}}$  may depend on the depth of the catalogue.) Depending on the mass spectrum considered, the redshift dependence of  $b_{\text{eff}}^2$  can be such as to partially or even completely balance the evolution of the mass autocorrelation function. The behaviour of  $b_{\text{eff}}$  emerging from such a model can be well–fitted by using the relation

$$b_{\text{eff}}(z) = 0.41 + [b_{\text{eff}}(z=0) - 0.41](1+z)^\beta. \quad (35)$$

The resulting fitting parameters are reported in Table 1 for our choice of initial matter fluctuation spectrum. One important feature of this model is that specifying a minimum mass for the objects determines their effective bias factor at  $z = 0$ . If the value required does not correspond to the empirically–determined bias parameter for any known class of objects then one must accept that such objects are transient and have faded sufficiently since the observed epoch to be missing from local redshift surveys. Alternatively, it may be that observational selection effects make objects visible at high redshift, but invisible at small distances, such as might be the case for extended objects of low surface brightness. We shall call this the *transient model* in the following discussion.

An alternative scenario based on these considerations is to fix the effective bias parameter at  $z = 0$  so that it agrees with a known population of present–day objects using  $b_0 = b_{\text{eff}}(0) \approx 1/\sigma_8^{nl} \approx 1.46$  – where by  $\sigma^{nl}$  we mean the non–linearly evolved *rms* mass fluctuation – and evolving it as

$$b_{\text{eff}}(z) = b_{-1} + (b_0 - b_{-1})(1+z)^\beta, \quad (36)$$

with suitable parameters  $b_{-1} \equiv b(z \rightarrow -1)$  and  $\beta$ ; fixing  $b_0$  effectively determines  $M_{\text{min}}$  while the previous calculation fixed  $M_{\text{min}}$  in order to determine  $b_0$ . If one therefore imagines that a given population of objects at the present epoch

[tp]

**Table 1.** The fitting parameters of the effective bias  $b_{\text{eff}}$  by using equation (35). Column 1: the minimum cutoff mass (in  $h^{-1} M_{\odot}$ ). Column 2: the value of  $b_{\text{eff}}$  at  $z = 0$ . Column 3: the parameter  $\beta$ .

$M_{\text{min}}$	$b_{\text{eff}}(z = 0)$	$\beta$
$10^9$	0.50	$1.92 \pm 0.01$
$10^{10}$	0.55	$1.89 \pm 0.01$
$10^{11}$	0.67	$1.85 \pm 0.01$
$10^{12}$	0.90	$1.79 \pm 0.01$
$10^{13}$	1.41	$1.76 \pm 0.02$
$10^{14}$	2.67	$1.78 \pm 0.03$

(with a ‘known’ value of  $b_0$ ) form via the merging of lower mass haloes, such as is the case in hierarchical clustering models, then this model would appear to be appropriate. For short we shall call this *merging model* in the subsequent discussion.

The crucial difference between the transient model and the merging model is that the latter requires that one identify the population of objects one is observing at high  $z$  with the progenitors of present-day bright galaxies while the former does not.

Our final alternative is motivated by different arguments. According to Nusser & Davis (1994) and Fry (1996), if galaxies form at some characteristic redshift  $z_f$  by some non-linear process which induces a bias parameter at that epoch  $b_f$  and if their subsequent motion is purely caused by gravity, then continuity leads to a redshift-dependent bias factor which evolves approximately as

$$b(z) = 1 + (b_f - 1) \frac{1+z}{1+z_f}, \quad z < z_f, \quad (37)$$

for  $\Omega_0 = 1$ . The obvious consequence of this simple model is that the bias factor always tends to unity as time goes on. Allowing for some spread in the values of  $b_f$  and  $z_f$ , depending e.g. on the mass of the galaxy, would not greatly change this evolution law. We call this model the *object-conserving model*. Equation (37) is consistent with the Mo & White (1995) formula, equation (33), provided that the effect of merging is negligible.

A linear dependence on  $1+z$  as obtained in the object-conserving model would also be obtained if objects were assumed to form at high peaks of the linear density field above some threshold  $\delta_c = \nu\sigma_{\text{lin}}$  threshold, with fixed  $\nu$  in accordance with equation (33). This model has been recently adopted by Croom & Shanks (1996) to fit the quasar two-point function.

Notice that all four of these models can be thought of as special cases of the merging model whose behaviour is described by equation (36). The transient model has its parameters fixed by the choice of halo mass cutoff. The merging model has parameters determined by the choice of bias parameter at  $z = 0$ . The object conserving model has  $b_{-1} = \beta = 1$ , but otherwise free parameters. The case  $b = 1$  for all epochs can also be accommodated by equation (36): a bias of unity in a merging model would occur if objects preferentially formed in haloes with mass close to  $M_*$  or if, for some reason, such objects were selected observationally.

These models are not exhaustive of all the possibilities, but they do serve to illustrate the spread in possible behaviours expected with fairly minimal assumptions about the bias. Alternative biasing models, not discussed further in this paper, have been considered by, for example, Coles (1993) who discusses a general class of local bias models and Catelan et al. (1994), who define a *weighted bias* algorithm, according to which the biased density field coincides with the mass-density whenever the latter exceeds some fixed threshold. As mentioned in Section 2, ‘generic’ local bias models predict that  $b$  is a function of scale, a fact we shall ignore in this analysis. This introduces the possibility that the *shape* as well as the amplitude of the biasing relation changes with epoch, allowing for an even wider range of possibilities. We shall defer this question to future work.

## 5 APPLICATIONS

In this section we illustrate the use of our formalism by applying it to a example data sets. Given the mass autocorrelation function, each class is characterized by *i*) its redshift distribution  $\mathcal{N}(z)$ , which automatically accounts for the catalogue selection function, and *ii*) the effective bias parameter  $b_{\text{eff}}(z)$  which we discussed in the previous Section. Note that our method is semi-empirical, in the following sense: the theoretical mass-function is only employed as the appropriate weighting factor to deduce the effective bias factor, but we never require that it predicts the observed

redshift distribution of objects in the catalogue, modulo the selection function; in our applications, in fact, we will take  $\mathcal{N}(z)$  as obtained from the data.

### 5.1 Spatial QSO correlation function

Quasars are a class of objects to which we may apply this formalism. Various authors have looked at the spatial quasar clustering and at their redshift evolution (e.g. Shanks et al. 1987; Iovino & Shaver 1988; Andreani & Cristiani 1992; Andreani et al. 1994; Shanks & Boyle 1994; Croom & Shanks 1996).

According to Efstathiou & Rees (1988), Haehnelt (1993) and Katz et al. (1994), every halo of mass greater than some threshold  $M_{\min} \sim 10^{11} - 10^{12} h^{-1} M_{\odot}$  harbours a QSO with a lifetime  $t_Q$  which we can assume to be much less than the time it takes for the halo to lose its identity by merging. In this case QSOs existing at a particular epoch sparsely sample the distribution of haloes with mass greater than  $M_{\min}$  at that epoch. This implies that  $b_{\text{eff}}(z)$  for quasars can be calculated using the transient model.

The spatial correlation function of quasars in the redshift range  $0.3 < z < 2.2$  is shown in the upper panel of Fig. 3; the redshift distribution  $\mathcal{N}(z)$  for the Durham/AAT survey is taken from Shanks & Boyle (1994) while the observational data are the updated estimates from Croom & Shanks (1996). The effective bias  $b_{\text{eff}}(z)$  is calculated from equation (16), where  $\bar{n}(z, M)$  is modelled by the Press–Schechter mass–function, with cutoff mass in the range  $10^{11} - 10^{12} h^{-1} M_{\odot}$ . As it is clear from the plot, given the uncertainty on the minimum mass of haloes able to host a quasar, our CDM–like model accounts for all the observational data, with the (possible) exception of the point at  $\approx 5h^{-1}$  Mpc, at which the difference is less than  $2\sigma$ .

In the other panels of Fig. 3 we plot the spatial correlation function of the same QSO catalogue in two different redshift ranges:  $0.3 < z < 1.4$  (centre) and  $1.4 < z < 2.2$  (bottom). While the results at higher redshifts are in good agreement with the observational data, the points at  $r \sim 10$  and at  $r \geq 20h^{-1}$  Mpc for  $0.3 < z < 1.4$  show a  $2\sigma$  deviation. Notice that the predicted evolution of  $\xi$  over these ranges is rather small, even for the upper band of the shaded region. In fact, the data at these scales suggest stable clustering in comoving coordinates. The possible discrepancies between the model and the data, however, are on very small scales, where  $\xi_{\text{obs}} > 1$ . This suggests that a more decisive test of this model could be constructed by quantifying the clustering of QSOs on scales smaller than  $r_c$ . Notice that there is some indication that a scale–dependent bias is required to reconcile the observed correlation function with that predicted by our model, but that this is to some extent predicted by realistic biasing scenarios (Coles 1993).

### 5.2 Angular and projected galaxy correlation functions

While the choice of bias model seems relatively straightforward for QSOs, this is not the case for galaxies. Various plausible arguments can be made for choosing any of the models we discussed in Section 4.

The first possibility we consider is that galaxies represent at *any* redshift an unbiased sample of the mass distribution, i.e. that  $b_{\text{eff}}(z) = 1$ . According to the model of equation (33), for the bias of dark matter haloes this situation would occur if galaxies were preferentially formed from haloes with mass close to  $M_{\star}(z_f)$  and survived until the epoch  $z$ .

Another possibility would be that faint galaxies are subunits that merge to make up more luminous galaxies (Broadhurst, Ellis & Glazebrook 1992; Clements & Couch 1996; Baugh, Cole & Frenk 1996), in which case, using the redshift dependence of  $b_{\text{eff}}(z)$  obtained in the previous section for dark matter haloes, looks a sensible choice. This model too fits into equation (36), for  $b_{-1} = 0.41$ ,  $b_0 = 1/\sigma_8^{n_l} \simeq 1.46$  and  $\beta \approx 1.8$ .

One might also assume that faint galaxies form a transient population of dwarf galaxies which has now faded away (Babul & Rees 1992; Lacey et al. 1993). This would motivate the transient model which, as we have noted, can also be described by equation (36). For illustrative purposes we incorporate a minimum mass of  $M_{\min} = 10^{11} h^{-1} M_{\odot}$ , with consequent values of the parameters given in Table 1.

If galaxies form at some particular redshift and then evolve without losing their identity and thus simply following the continuity equation thereafter, the object–conserving model seems to be appropriate. In this picture, faint galaxies of a particular type would be identified with ‘ordinary’ luminous galaxies at high redshift (e.g. Tyson 1988). It is natural to apply this scenario to, for example, present-day bright spirals which appear to have survived undisturbed for some time by interactions or mergers with objects of a similar mass: the corresponding value of  $b_0 = 1/\sigma_8^{n_l} \simeq 1.46$ .

Given the plausibility of each of these models, we now compare all of them with the best currently available data on the evolution of galaxy clustering with redshift using the model described in Section 2 to evolve the underlying matter correlations.

In the top panel of Fig. 4 we plot the angular correlation of galaxies out to  $z = 1.6$  for the Canada–France Redshift Survey (CFRS). The galaxy redshift distribution is taken from Crampton et al. (1995). The observational

data have been obtained by Hudon & Lilly (1996) and refer to the same catalogue. These data are uncorrected for the integral constraint, spurious field to field variations or for stellar contamination. Two different methods were used by Hudon & Lilly to estimate  $\omega(\theta)$  from the observational data: in the first the angular correlation is obtained by averaging the different estimates in each of the 24 fields composing the catalogue (local method, open circles); in the second the counting of pairs is done over all cells in the sample (global method, filled squares). The true unbiased angular correlation is bracketed by the two methods.

The bottom panel of the same figure shows our prediction for a sample of 222 galaxies with  $z \leq 1.6$  selected from the Hawaii Keck K-band survey (Cowie et al. 1996). The redshift distribution  $\mathcal{N}(z)$  and the correlation data are taken from Carlberg et al. (1996). In order to take into account the dilution produced by the uncorrelated foreground stars, we correct the original data by a factor of  $(1 - f_*)^{-2}$ , where  $f_*$  is the fraction of catalogued objects that are stars. Carlberg et al. (1996) estimate for their catalogue  $f_* = 1/4$ .

Note that the CFRS data are well described by both the unbiased and transient model while the Keck data, with their larger errors, are compatible with the galaxy-conserving model and, marginally, with the merging model.

In Fig. 5 we present our prediction for galaxies in the Hubble Deep Field (HDF). Villumsen, Freudling & da Costa (1996) fit the redshift distribution by

$$\mathcal{N}(z) = 2.723 \frac{z^2}{z_0^3} \exp[-(z/z_0)^{2.5}] , \quad (38)$$

where  $z_0$  is approximately the median redshift. Alternative estimates of the redshift distribution for these galaxies are presented by Lanzetta, Yahil & Fernández-Soto (1996), but for illustrative purposes we adopt the former results here. We consider four samples with magnitude limits  $R = 26, 27, 28, 29$ , with corresponding median redshifts of  $z_0 = 1.35, 1.54, 1.71, 1.87$ , respectively. Observational estimates of the correlation functions for these samples have also been obtained by Villumsen, Freudling & da Costa (1996). After correcting the results to include the integral constraint, they fitted their angular correlations by assuming a power law

$$\omega(\theta) = A\theta^{-\delta} \quad (39)$$

with fixed slope  $\delta = 0.8$ . The shaded region in the plots refers to the  $1\sigma$  range allowed by their fits.

Again the unbiased model appears to provide the best fit over all the the samples selected: the other biasing models yield too high an amplitude for the deeper samples. There is also some indication that the actual correlation function of galaxies in this catalogue is steeper than the model predicts, though this may in principle be accounted for by allowing the bias factor to depend on scale in the expected fashion (Coles 1993).

In Fig. 6 we plot the projected correlation function for galaxies with CFRS redshift distribution and compare it with observational data from the same catalogue (Le Fèvre et al. 1996). The data are divided in three ranges in redshift:  $0.2 < z < 0.5$ ,  $0.5 < z < 0.75$  and  $0.75 < z < 1$ . Note that the observational data, originally plotted as a function of the proper projected separation at the median redshift of three considered strips ( $z = 0.34$ ,  $z = 0.62$  and  $z = 0.86$  respectively), have been rescaled to the comoving, projected separation  $r_p$ . Again the merging model and the number-conserving model overpredict the correlations, and the overprediction is worse for the samples at higher  $z$ . The unbiased and transient models are, however, good fits to the data.

Fig. 7 shows our prediction for galaxies for the Keck sample, with redshift distribution and correlation data from Carlberg et al. (1996). Two different strips are here considered:  $0.3 < z < 0.9$  and  $0.9 < z < 1.5$ . Observational data are rescaled as before at the median redshift,  $z = 0.6$  and  $z = 1.1$  respectively. Again the merging model seems to be excluded by the high redshift data; the other three alternatives are consistent. Again, there is some evidence that, at high redshift, the shape of the galaxy correlation function is wrong, possibly because of scale-dependence of  $b$ .

## 6 CONCLUSIONS

The principal result of this analysis is that uncertainties in the evolution of the bias parameter with epoch  $z$  are potentially the dominant consideration to be taken into account when testing theoretical models against galaxy clustering evolution data. Looking at this in another way, one can say that the rough consistency of observed clustering data at high redshift with unbiased models can place strong constraints on the bias invoked in any particular theory of structure formation. One has to be very careful about postulating a significant bias at  $z = 0$  without thinking carefully about how the bias was introduced, as plausible scenarios give a bias parameter that evolves strongly with cosmic epoch in contrast with the observations. Since all the bias models we consider can be described by the same formula (36), this basically argues that, at least within the class of models considered, the bias must be small at the present epoch so as not to increase too drastically with redshift. Notice further that any extra correlations introduced by the effects of magnification bias induced by gravitational lensing actually strengthen this conclusion, as the observed clustering must include both the intrinsic clustering of the objects and the contribution from correlated shear.

In the case of QSOs, we find that a simple model in which quasars trace the distribution of haloes is roughly consistent with the clustering data supplied by Croom & Shanks (1996) for all epochs. This conclusion contrasts with the claim of Croom & Shanks that the apparently low level of clustering evolution requires either a strong bias or a low density universe (or both). The important points of disagreement with Croom & Shanks (1996) are that (i) their conclusions are based on a standard CDM model (i.e.  $\Gamma_{\text{eff}} = 0.5$ ) for the initial power-spectrum, (ii) they use linear theory to evolve the matter fluctuations and (iii) they adopt a model for the evolution of bias which resembles our object-conserving model.

It is pertinent to compare our analysis of galaxy clustering data with a recent paper by Peacock (1996). By comparing estimates of the power-spectrum of clustering at  $z = 0$  and the CFRS data on redshift evolution with the expected non-linear evolution of a phenomenological model for the power-spectrum he concludes that only an unbiased model for galaxy correlations in a low density universe is compatible with the observations. We have not studied low-density models in this paper, so we do not comment on whether such models offer a better explanation of the power-spectrum. There are, however, some important points of difference between our analysis of Einstein-de Sitter models and that of Peacock (1996). First, the model for the initial power-spectrum adopted by Peacock is of a slightly different form to ours: he uses a model of two power laws with a transition region in between. Since our model is not exactly a power law on small scales there will be some differences in the consequent clustering behaviour starting from these two different initial assumptions. These differences might well alter the behaviour of the correlation function on the relatively small scales where its amplitude is known accurately. Secondly, Peacock (1996) uses a different fitting formula for the non-linear evolution of correlations, based on that of Peacock & Dodds (1996). Third, Peacock (1996) does not consider models for the evolution of  $b$ , preferring instead to assume that the bias factor has the same value at all redshifts. Finally, we do not include clustering data obtained from catalogues at zero redshift in our analysis because different surveys may either involve physically different objects or possess different observational selection functions (or both).

These differences are important when we compare our main conclusion (that unbiased or mildly biased clustering developing from our initial spectrum in a universe with  $\Omega_0 = 1$  is consistent with the clustering data) with Peacock's conclusion that he cannot reproduce the observed clustering with his model in a universe with  $\Omega_0 = 1$  unless he invokes a particular form of biasing to counteract the small-scale evolution of the matter power-spectrum. Since the differences in our approaches manifest themselves most strongly on small scales, these are probably the origin of our disagreement on this point. In any case, we do not attempt to fit the detailed shape of the IRAS/APM power-spectrum (for reasons mentioned above) and this is his main argument that a specific form of the bias is necessary if  $\Omega_0 = 1$ . The CFRS and Keck data, in themselves, are well explained by our model. Nevertheless, it is obviously important to understand the origin of present-day bright galaxies such as those constituting the APM survey. It emerges from our analysis that there is a problem explaining the high value of  $b_0 \simeq 1.4$  required by our CDM-like model for the these galaxies. According to the models we have presented, a population of present-day objects with  $b_0 > 1$  should be identifiable with some class of high-redshift objects with an even higher value of  $b$ , unless the present-day objects are contained within haloes having a minimum mass of order  $10^{13} M_{\odot}$  (see Fig. 2) and which is very different from that corresponding to any observable high-redshift objects. An alternative solution to this conundrum that does not require a 'special' population of objects to be identified with present-day galaxies is to invoke  $\Omega_0 < 1$ , because then there is no need for bright galaxies at the present epoch to have  $b_0 > 1$ . A model with  $\Omega_0 < 1$  and in which bright galaxies trace the mass is probably consistent with both the high-redshift data and local measures of clustering, as argued by Peacock (1996).

The discrepancies between our conclusions for both QSOs and galaxies and the studies of Croom & Shanks (1996) and Peacock (1996) respectively, serve as an important reminder of the model-dependence of this type of analysis and of some of the residual theoretical uncertainties. In particular, it is important to understand the small-scale stable clustering limit in more detail if this technology is to be improved. Above all, however, we need to develop much better defined models for the form and evolution of biasing in a general context, for even in the simplest case in which the bias is a constant linear multiplier there is considerable ambiguity in the modelling of its evolution.

## ACKNOWLEDGMENTS.

We would like to thank P. Andreani for useful discussions, B. Jain for detailed explanations of a number of technical points and J. Peacock for his very helpful advice. R.G. Carlberg, S.M. Croom, O. Le Fèvre and T. Shanks are warmly thanked for providing us electronic versions of their results. Italian MURST is acknowledged for partial financial support. PC is a PPARC Advanced Research Fellow; he would like to thank the Department of Astronomy in Padova for their hospitality during a visit. SM would like to thank QMW for hospitality under the PPARC Visitors grant.

## REFERENCES

- Andreani P., Cristiani S., 1992, *ApJ*, 398, L13
- Andreani P., Cristiani S., Lucchin F., Matarrese S., Moscardini L., 1994, *ApJ*, 430, 458
- Babul A., Rees M.J., 1992, *MNRAS*, 255, 346
- Bagla J.S., Padmanabhan T., 1994, *MNRAS*, 266, 227
- Bagla J.S., Padmanabhan T., 1996, preprint astro-ph/9605202
- Bardeen J.M., Bond J.R., Kaiser N., Szalay A.S., 1986, *ApJ*, 304, 15
- Baugh C.M., Gaztañaga E., 1996, *MNRAS*, 280, L37
- Baugh C.M., Cole S., Frenk C.S., 1996, preprint astro-ph/9607056
- Bennett C.L. et al., 1996, *ApJ*, 464, L1
- Bernstein G.M., Tyson J.A., Brown W.R., Jarvis J.F., 1994, *ApJ*, 426, 526
- Brainerd T.G., Villumsen J.V., 1994, *ApJ*, 431, 477
- Brainerd T.G., Scherrer R.J., Villumsen J.V., 1993, *ApJ*, 418, 570
- Brainerd T.G., Smail I., Mould J., 1995, *MNRAS*, 275, 781
- Broadhurst T.J., Ellis R.S., Glazebrook K., 1992, *Nat*, 355, 55
- Bunn E.F., White M., 1996, astro-ph/9607060
- Carlberg R.G., Cowie L.L., Songaila A., Hu E.M., 1996, preprint astro-ph/9605024
- Catelan P., Coles P., Matarrese S., Moscardini L., 1994, *MNRAS*, 268, 966
- Clements D.L., Couch W.J., 1996, *MNRAS*, 280, L43
- Cole S., Kaiser N., 1989, *MNRAS*, 237, 1127
- Cole S., Ellis R., Broadhurst T., Colless M., 1994, *MNRAS*, 267, 541
- Coles P., 1993, *MNRAS*, 262, 1065.
- Coles P., 1996, *Contemporary Physics*, in press.
- Coles P., Ellis G.F.R., 1996, *Is the Universe Open or Closed?*, Cambridge University Press, Cambridge.
- Colín P., Carlberg R.G., Couchman H.M.P., 1996, preprint astro-ph/9604071
- Couch W.J., Jurcevic J.S., Boyle B.J., 1993, *MNRAS*, 260, 241
- Cowie L.L., Songaila A., Hu E.M., Cohen J.G., 1996, *AJ*, submitted
- Crampton D., Le Fèvre O., Lilly S.J., Hammer F., 1995, *ApJ*, 455, 96
- Croom S.M., Shanks T., 1996, *MNRAS*, in press
- Davis M., Peebles P.J.E., 1983, *ApJ*, 267, 465
- Efstathiou G., 1995, *MNRAS*, 272, L25
- Efstathiou G., Rees M.J., 1988, *MNRAS*, 230, 5p
- Efstathiou G., Bond J.R., White S.D.M. 1992, 258, 1P
- Efstathiou G., Bernstein G., Katz N., Tyson J.A., Guhathakurta P., 1991, *ApJ*, 380, L47
- Efstathiou G., Frenk C.S., White S.D.M., Davis, M., 1988, *MNRAS*, 235, 715
- Fixsen D.J., Cheng E.S., Gales J.M., Mather J.C., Shafer R.A., Wright E.L., 1996, preprint astro-ph/9605054
- Fry J.N., 1996, *ApJ*, 461, L65
- Górski K.M., Banday A., Bennett C.L., Hinshaw G., Kogut A., Smoot G.F., Wright E.L., 1996, *ApJ*, 464, L11
- Gurbatov S.N., Saichev A.I., Shandarin S.F., 1989, *MNRAS*, 236, 385
- Haenhelt M.G., 1993, *MNRAS*, 265, 727
- Hamilton A.J.S., Kumar P., Lu E., Mathews A., 1991, *ApJ*, 374, L1
- Hudon J.D., Lilly S.J., 1996, preprint astro-ph/9605056
- Iovino A., Shaver P., 1988, *ApJ*, 330, L13
- Jain B., 1996, preprint astro-ph/9605192
- Jain B., Bertschinger E., 1996, *ApJ*, 456, 43
- Jain B., Mo H.J., White S.D.M., 1995, *MNRAS*, 276, L25
- Kaiser N., 1984, *ApJ*, 284, L9
- Katz, N., Quinn, T., Bertschinger, E., Gelb, J.M., 1994, *MNRAS*, 270, L71
- Lacey C., Guiderdoni B., Rocca-Volmerange B., Silk J., 1993, *ApJ*, 402, 15
- Lanzetta K.M., Yahil A., Fernández-Soto A., 1996, *Nature*, 381, 759
- Le Fèvre O., Hudon D., Lilly S.J., Crampton D., Hammer F., Tresse L., 1996, *ApJ*, 461, 534
- Matarrese S., Lucchin F., Moscardini L., Saez D., 1992, *MNRAS*, 259, 437
- Melott A.L., 1992, 393, L45
- Mo H.J., White S.D.M., 1995, *MNRAS*, in press, preprint astro-ph/9512127
- Mo H.J., Jing Y.P., White S.D.M., 1996, preprint astro-ph/9602052
- Munshi D., Padmanabhan T., 1996, preprint astro-ph/9606170
- Neuschaefer L.W., Windhorst R.A., Dressler A., 1991, *ApJ*, 382, 32
- Nityananda R., Padmanabhan T., 1994, *MNRAS*, 271, 976
- Nusser A., Davis M., 1994, *ApJ*, 421, L1
- Osmer P.S., 1981, *ApJ*, 247, 762
- Padmanabhan T., 1996, *MNRAS*, 278, L29
- Padmanabhan T., Cen R., Ostriker J.P., Summers F.J., 1996, *ApJ*, in press
- Peacock J.A., 1996, preprint.
- Peacock J.A., Dodds S.J., 1994, *MNRAS*, 267, 1020
- Peacock J.A., Dodds S.J., 1996, *MNRAS*, 280, L19
- Peebles P.J.E., 1980, *The large-scale structure of the Universe*. Princeton University Press, Princeton
- Press W.H., Schechter P., 1974, *ApJ*, 187, 425

- Roche N., Shanks T., Metcalfe N., Fong R., 1993, MNRAS, 263, 360  
Roche N., Shanks T., Metcalfe N., Fong R., 1996, MNRAS, 280, 397  
Sahni V., Coles, P., 1995, Phys. Rep., 262, 1  
Shanks T., Boyle B.J., 1994, MNRAS, 271, 753  
Shanks T., Fong R., Boyle B.J., Peterson B.A., 1987, MNRAS, 227, 739  
Shepherd C.W., Carlberg R.G., Yee H.K.C., Ellingson E., 1996, preprint astro-ph/9601014  
Sheth R., Jain B., 1996, preprint astro-ph/9602103  
Stebbins A., Caldwell R.R., 1995, Phys. Rev. D, 52, 3248.  
Sugiyama N., 1995, ApJS, 100, 281  
Turner E.L., 1980, ApJ, 349, L19  
Tyson J.A., 1988, AJ, 91, 1  
Villumsen J.V., 1995, preprint astro-ph/9512001  
Villumsen J.V., Freudling W., da Costa L.N., 1996, preprint astro-ph/9606084  
Weinberg S., 1972, Gravitation and cosmology. J. Wiley & Sons, New York  
White M., Viana P.T.P., Liddle A.R., Scott D., 1996, MNRAS, in press, preprint astro-ph/9605057  
Zel'dovich Ya.B., 1970, A&A., 5, 84

**FIGURE CAPTIONS**

**Figure 1.** The mass autocorrelation function  $\xi$  as a function of the comoving separation  $r$ , at different redshifts:  $z = 3$  (top left),  $z = 2$  (top right),  $z = 1$  (bottom left) and  $z = 0$  (bottom right). Different lines refer to different models for the clustering evolution: JMW fitting formula (solid line), linear theory (dotted line) and stable clustering (dashed line).

**Figure 2.** The effective bias  $b_{\text{eff}}$  as a function of the redshift  $z$ . Different lines refer to different values of the minimum mass in the Press–Schechter mass–function, ranging from  $10^9$  to  $10^{14} h^{-1} M_{\odot}$ , from bottom to top.

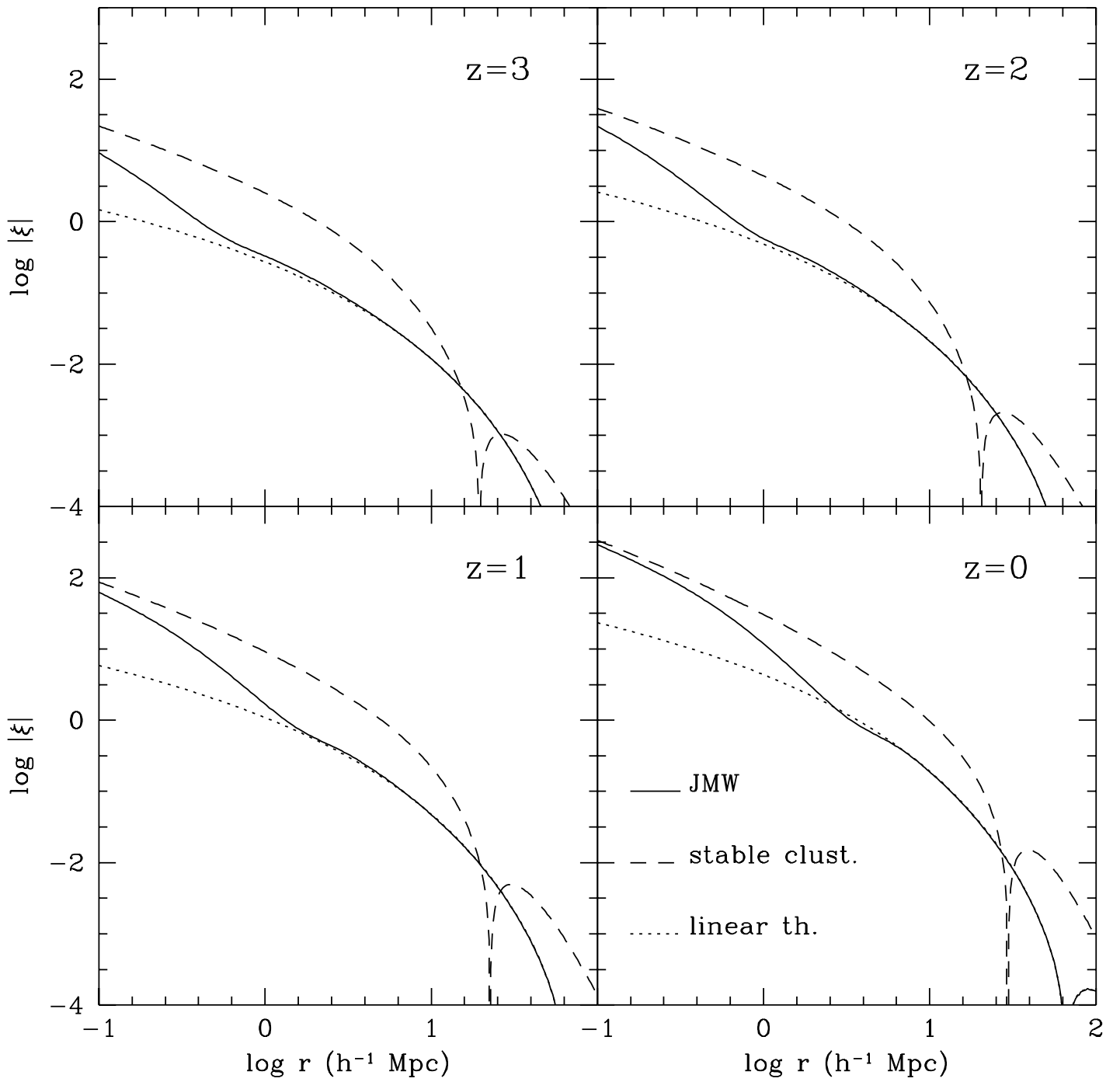
**Figure 3.** Theoretical prediction for the spatial correlation function of quasars, with  $\mathcal{N}(z)$  given by the Durham/AAT redshift distribution (Shanks & Boyle 1994). Different panels refer to different redshift ranges: whole range  $0.3 < z < 2.2$  (top),  $0.3 < z < 1.4$  (centre) and  $1.4 < z < 2.2$  (bottom). The shaded region shows the values obtained if the effective bias is obtained with a minimum mass in the band  $M_{\text{min}} = 10^{11}$  (lower line) and  $10^{12} h^{-1} M_{\odot}$  (upper line). The open squares and relative error bars refer to the Croom & Shanks (1996) results for the observed QSO two–point function in the same sample.

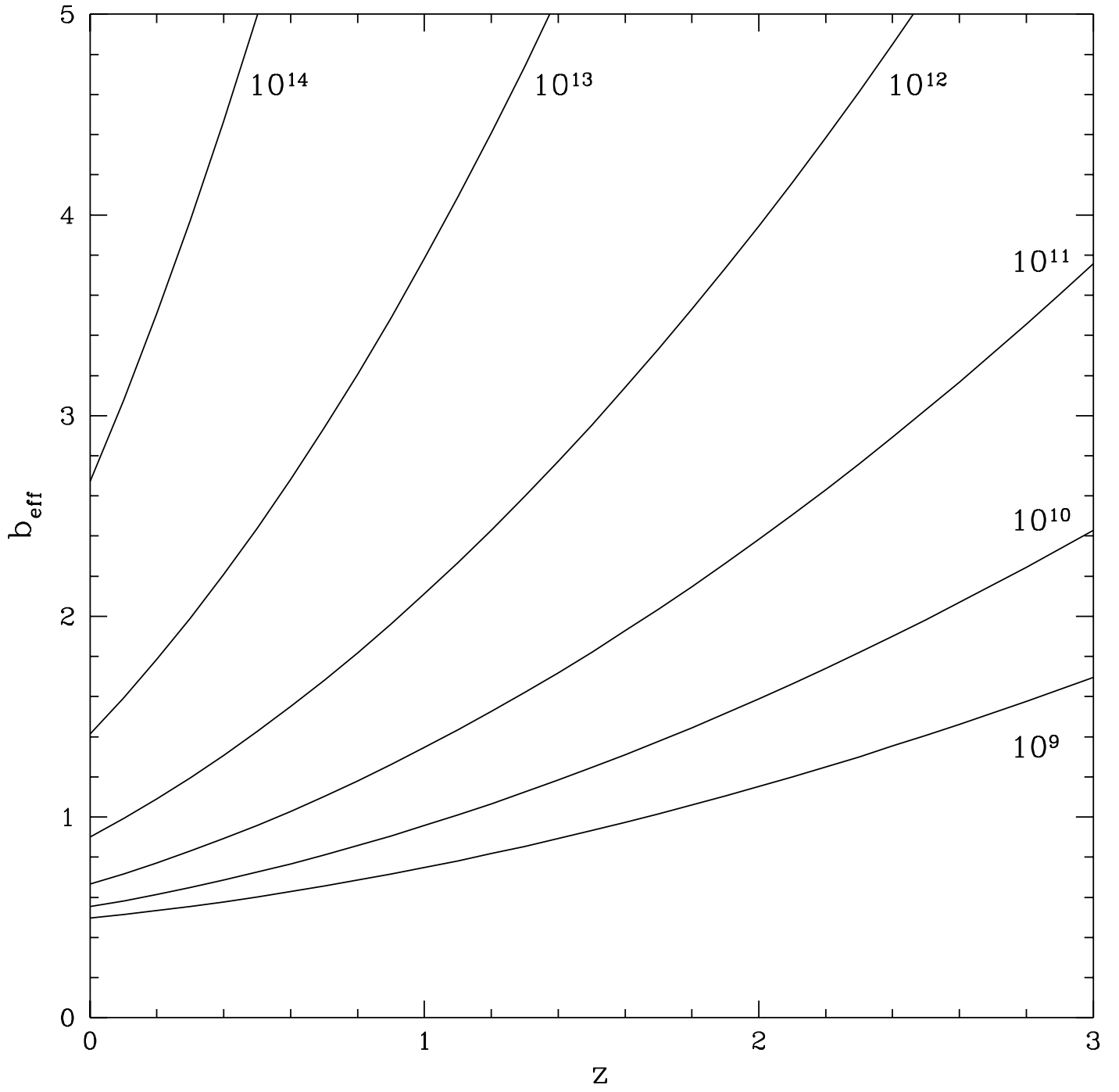
**Figure 4.** Theoretical prediction for the angular galaxy correlation function. Top panel: galaxies with  $z < 1.6$  and  $\mathcal{N}(z)$  given by the CFRS redshift distribution (Crampton et al. 1995). Correlation data are from Hudon & Lilly (1996) and are obtained by using two different methods which bracket the true values: the local and global determinations are shown by open circles and filled squares, respectively. Bottom panel: galaxies in the redshift range  $0 < z < 1.6$  selected from the Hawaii Keck K–band survey, with redshift distribution and correlation data from Carlberg et al. (1996). The original data are corrected to take into account the dilution produced by the uncorrelated foreground stars. Different bias models are considered: unbiased model [ $b(z) = 1$ ; solid line]; galaxy–conserving model [equation (36) with  $b_0 = 1.46$ ,  $b_{-1} = \beta = 1$ ; dotted line]; merging model equation (36) with  $b_0 = 1.46$ ,  $b_{-1} = 0.41$  and  $\beta = 1.8$ ; short dashed line]; transient model [equation (36) with  $b_0 = 0.67$ ,  $b_{-1} = 0.41$ ,  $\beta = 1.85$ ; long dashed line]. The latter model almost coincides with the unbiased case.

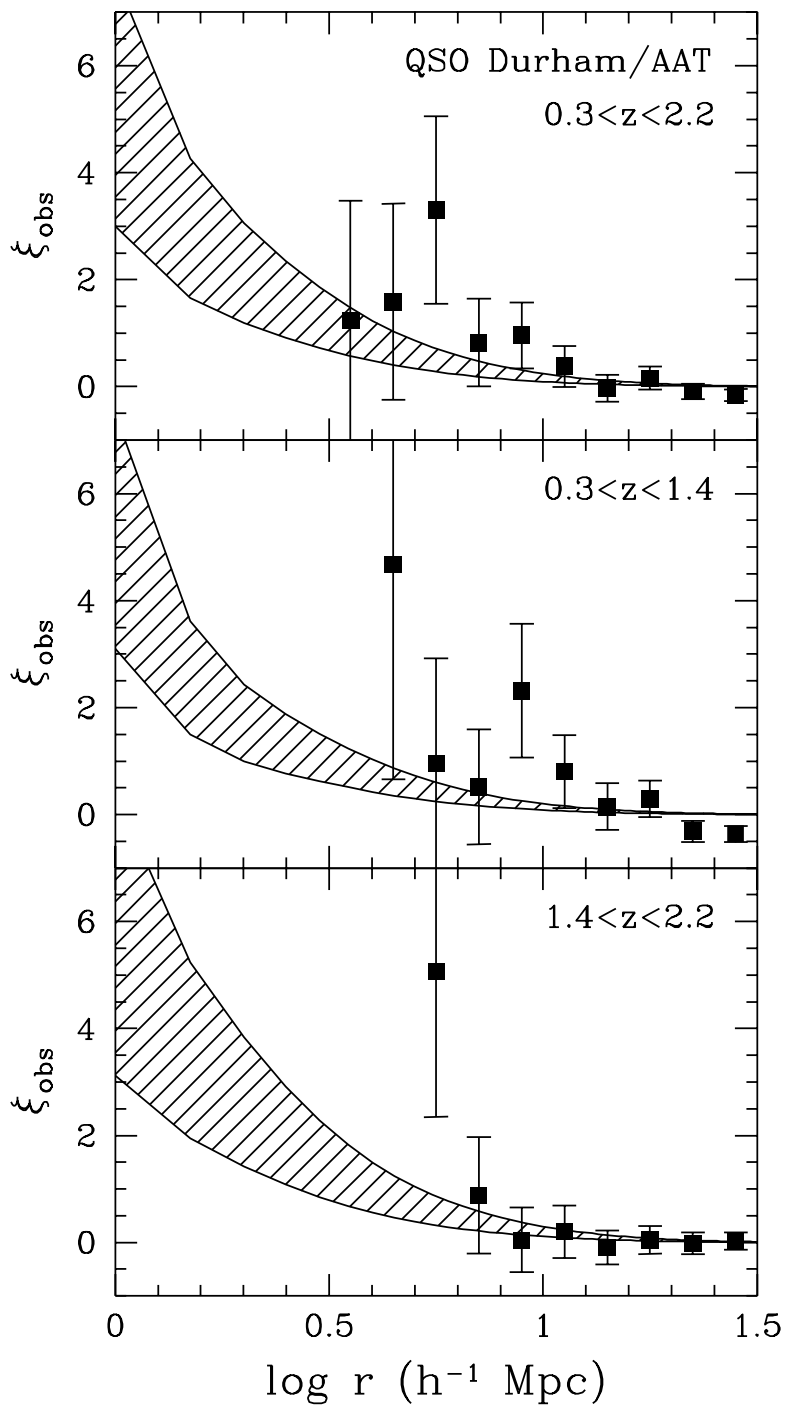
**Figure 5.** Theoretical prediction for the angular galaxy correlation function for the Hubble Deep Field. The shaded region in the plots refers to the  $1\sigma$  range allowed by the fit obtained on the observational data by Villumsen, Freudling & da Costa (1996). The panels show the results for four  $R$  magnitude limited samples with different median redshift  $z_0$ :  $R < 26$  and  $z_0 = 1.35$  (top left),  $R < 27$  and  $z_0 = 1.54$  (top right),  $R < 28$  and  $z_0 = 1.71$  (down left) and  $R < 29$  and  $z_0 = 1.87$  (down right). Different bias models are shown as in Fig. 4.

**Figure 6.** Theoretical prediction for the projected galaxy correlation function of the CFRS sample. The redshift distribution is given by Crampton et al. (1995). Correlation data are from Le Fèvre et al. (1996). Different panels refer to different strips in redshift:  $0.2 < z < 0.5$  (top),  $0.5 < z < 0.75$  (centre) and  $0.75 < z < 1$  (bottom). Different bias models are shown as in Fig. 4.

**Figure 7.** Theoretical prediction for the projected galaxy correlation function of the Hawaii Keck K–band survey. The redshift distribution and correlation data are from Carlberg et al. (1996). Different panels refer to different strips in redshift:  $0.3 < z < 0.9$  (top) and  $0.9 < z < 1.5$  (bottom). Different bias models are shown as in Fig. 4; the transient model almost coincides with the  $b = 1$  (unbiased) model in the upper panel.







CFRS

Keck

